Thin Solid Films 594 (2015) 96–100

Contents lists available at ScienceDirect

Thin Solid Films

journal homepage: www.elsevier.com/locate/tsf

Optical properties of ultrathin Al_2O_3/ZnO nanolaminates

R. Viter [a,b], I. Baleviciute [c,d], A. Abou Chaaya [e], L. Mikoliunaite [c], Z. Balevicius [d,f], A. Ramanavicius [c,d], A. Zalesska [a], V. Vataman [a], V. Smyntyna [a], Z. Gertnere [g], D. Erts [g], P. Miele [e], M. Bechelany [e,*]

[a] Faculty of Physics, Experimental Physics Department, Odessa National I.I. Mechnikov University, 42, Pastera, 65026, Odessa, Ukraine
[b] Institute of Atomic Physics and Spectroscopy, University of Latvia, 19, Raina Blvd., LV 1586, Riga, Latvia
[c] Vilnius University, Faculty of Chemistry, Department of Physical Chemistry, Naugarduko 24, 03225 Vilnius 6, Lithuania
[d] Center for Physical Sciences and Technology, Laboratory of BioNanoTechnology, A. Gostauto 11, LT-01108 Vilnius, Lithuania
[e] Institut Europeen des Membranes, UMR 5635 ENSCM UM CNRS, Universite Montpellier, Place Eugene Bataillon, F-34095 Montpellier cedex 5, France
[f] Faculty of Electronics, Vilnius Gediminas Technical University, Sauletekio 11, LT-10223 Vilnius, Lithuania
[g] Institute of Chemical Physics, University of Latvia, 19, Raina Blvd., LV 1586, Riga, Latvia

ARTICLE INFO

Article history:
Received 25 May 2015
Received in revised form 8 September 2015
Accepted 8 October 2015
Available online xxxx

Keywords:
Atomic Layer Deposition
Amorphous nanolaminates
ZnO
Ultrathin films
Optical properties

ABSTRACT

Because of their high resistance against ultraviolet and high energy particles, ultrathin amorphous nanolaminates can be very attractive for aerospace application. Here we report on the optical and structural properties of ultrathin Al_2O_3/ZnO nanolaminates deposited by Atomic Layer Deposition. Structural properties of nanolaminates were studied by GIXRD and AFM. Optical characterization was performed by transmittance, spectroscopic ellipsometry and photoluminescence (PL) spectroscopy. Regression analysis of ellipsometric spectra has shown that absorption peak decreases and blue shifted with the decrease of bilayer thickness in the stack. On the basis of the analysis of structural and optical properties of ultrathin nanolaminates, the amorphous nature of them is suggested.

1. Introduction

Nowadays a new class of materials based on nanostructures is started to be use for innovative optical elements, [1] photovoltaic, energy storage devices [2] and temperature sensitive substrates for biosensors [3–6]. Nanolaminates have been applied for aerospace application as thin shell mirrors. Because of their high resistance against ultraviolet irradiation and high energy particles, ultrathin nanolaminates can be very attractive when amorphous structures are achieved [7].

It is well known that bulk and thin films of hundreds of nanometers of zinc oxide deposited on various substrates most frequently generate an anisotropic optical response to incident electromagnetic field. A number of publications have been dedicated for studies of anisotropic ZnO dielectric function in deep-ultra-violet, ultra-violet, visible and infrared regions [8]. However, ZnO layers with hexagonal crystal structure do not have necessary mechanical and optical features for advanced applications in the fields mentioned above. For this purpose, zinc oxide nanolaminates (about 2 nm and less) are one of the most prospective materials for such applications because their amorphous structures.

Optical methods such as transmittance-reflection spectroscopy, spectroscopic ellipsometry (SE) and photoluminescence spectroscopy (PL) can be very useful to characterize the structure of ultrathin nanolaminates. Transmittance-reflection spectroscopy indicates the changes of absorption for different thicknesses of nanolaminates bilayers. Optical dispersion of refractive index of ultrathin ALD deposited nanolaminates can determine optical parameters of individual layers in multilayered ultrathin structures. Large interface sensitivity of SE enables us to analyze in detail the structure and properties of ultrathin layers [9]. Spectra of PL give information about exitonic peak position and amplitude which is the indication of level of ordering in ZnO layers. They demonstrate room temperature photoluminescence in UV and visible range, corresponding to near band and defect level emission, respectively.

In the present work the optical methods studies have been carried out on ultrathin nanolaminates of Al_2O_3/ZnO layers (lower than 20 nm). The determined optical parameters of nanolaminates were analyzed in order to reveal amorphous structure of ultrathin ZnO layers. The most of attention was paid to absorption changes of transmittance and ellipsometric spectra with bilayers thickness decreasing in nanolaminates. The reasons of the observed effect were discussed. Here we focus more on the characterization of nanolaminates by spectroscopic optical methods such as optical transmission-reflection, spectroscopic ellipsometry and photoluminescence. We want to show that from spectroscopic optical methods, we can reliably characterize

* Corresponding author.
E-mail addresses: viter_r@mail.ru (R. Viter), mikhael.bechelany@univ-montp2.fr (M. Bechelany).

http://dx.doi.org/10.1016/j.tsf.2015.10.018
0040-6090/

Table 1
Thickness of ZnO single thin film and Al_2O_3/ZnO ultrathin nanolaminates synthesis by ALD.

Samples	Cycles of Al_2O_3	Cycles of ZnO	Numbers of bilayers	Bilayer thickness (nm)
Al_2O_3/ZnO 20 (0.6/0.6 nm)	3	3	20	1.2
Al_2O_3/ZnO 10 (1/1 nm)	5	5	10	2
Al_2O_3/ZnO 4 (2.6/2.6 nm)	13	13	4	5.2
Al_2O_3/ZnO 2 (5/5 nm)	25	25	2	10
Al_2O_3/ZnO 1 (10/10 nm)	50	50	1	20

the transition from crystalline to amorphous structures and evaluate the degree of disorder.

2. Experimental details

2.1. Materials

Diethyl Zinc (DEZ) ($Zn(CH_2CH_3)_2$, 95% purity, CAS: 557-20-0) and Trimethylaluminum (TMA) ($(CH_3)_3Al$) 98% purity, CAS: 75-24-1) were obtained from Sigma Aldrich. Silicon wafer p-type (100) and glass substrates were purchased from MEMC Korea Company and RS France respectively.

2.2. Synthesis of Al_2O_3/ZnO ultrathin nanolaminates

Silicon and glass substrates were pre-cleaned in acetone, ethanol and deionized water. A custom made ALD reactor was used for the synthesis of ultrathin Al_2O_3/ZnO nanolaminates. ALD was performed using sequential exposures of TMA (DEZ) and H_2O separated by a purge of argon with a flow rate of 100 sccm. The deposition regime for ZnO and Al_2O_3 consisted of 0.1 s pulse of TMA (DEZ), 30 s of exposure to TMA (DEZ), 30 s of purge with argon followed by 2 s pulse of H_2O, 30 s of exposure to H_2O and finally 40 s purge with argon. Al_2O_3/ZnO ultrathin nanolaminates with different number of cycles were deposited both on Si substrates and glass substrates by ALD (Table 1), the temperature was fixed to 100 °C.

2.3. Characterization

Structural properties of Al_2O_3/ZnO nanolaminates were characterized using Grazing Incidence X-ray Diffraction (GIXRD; Bruker D5000). BioScope Catalyst (Bruker, USA) atomic force microscope in contact mode was used for the evaluation of surface morphology. Sharpened silicon nitride tip (spring constant — 0.35 N/m, resonant frequency — 65 kHz) was employed. Surface roughness was calculated using NanoScope 8.10 software.

Optical properties of ultrathin nanolaminates have been studied by photoluminescence spectroscopy in the spectral range 370–800 nm. The excitation of luminescence was performed by a solid state laser source (Nd:YAG, LCS-DTL-374QT, Russia, 355 nm, 13 mW/cm^2). The registration of the emitted spectra was provided by an experimental setup described elsewhere [10,11].

All spectroscopic ellipsometry measurements were carried from 210 nm to 1000 nm wavelength using J. A. Woollam spectral ellipsometer M-2000× with a rotating compensator. Measurements of nanolaminates were performed at fixed angle of incident light 70°. For calculation of optical constants Complete Ease software from J. A. Woollam was used. Measurement procedure was performed in the same way as in our previous work [11].

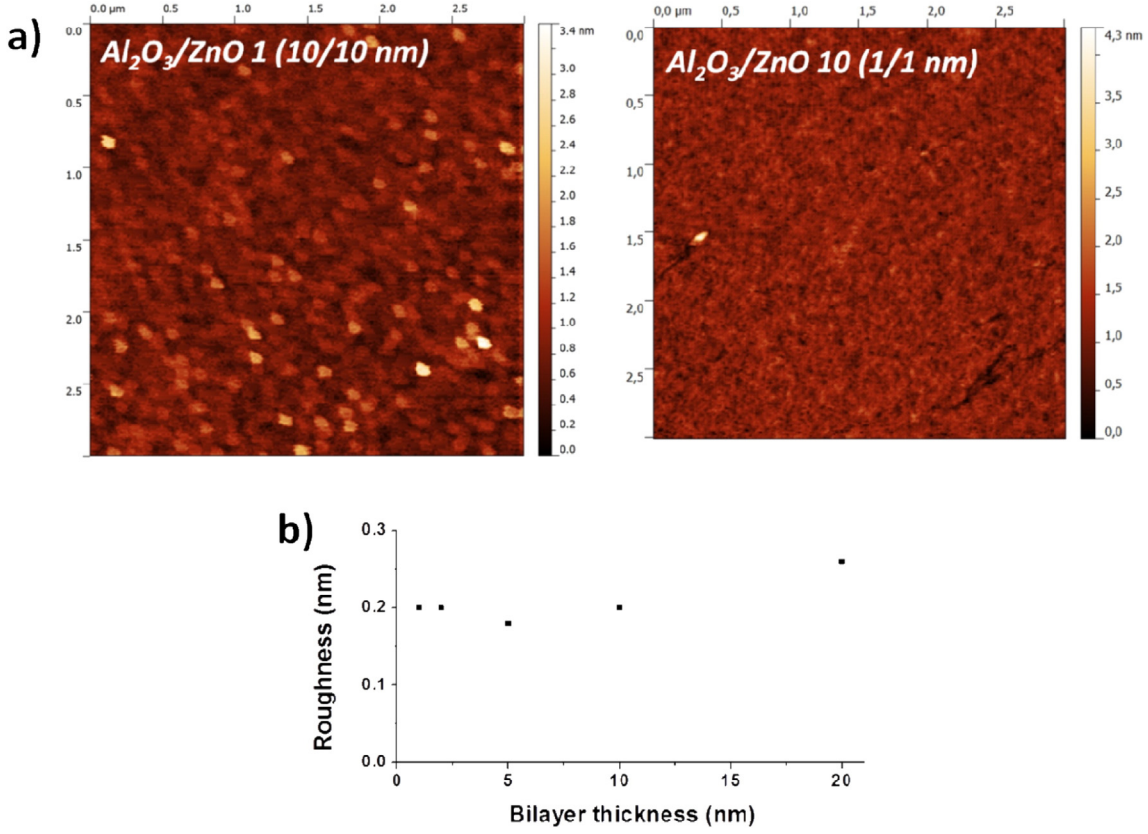

Fig. 1. (a) AFM images of Al_2O_3/ZnO nanolaminates with different bilayer thicknesses; the image size is 3 μm × 3 μm and the height scale is 4 nm; (b) roughness vs the bilayers thickness in the Al_2O_3/ZnO ultrathin nanolaminates.

3. Results and discussion

Al_2O_3/ZnO ultrathin nanolaminates (about 20 nm total thickness) with different bilayers thicknesses were deposited both on Si substrates and glass substrates by ALD (Table 1). In all ultrathin nanolaminates, the first layer on Si substrate was Al_2O_3 and the top layer of the nanolaminate was ZnO. The growth rates of Al_2O_3 and ZnO in the nanolaminates vary between 1.4 to 2 Å per cycle and 1.8 to 2 Å per cycle respectively as it has been determined elsewhere. In our previous study on structural and mechanical properties of Al_2O_3/ZnO nanolaminates, [12]we demonstrated that with bilayer spacing of 2.5 nm, the ZnO film becomes fully amorphous. Transition from crystalline to amorphous structure with the decrease of bilayer spacing was demonstrated by TEM and GIXRD [10,11,13].

Surface morphology of the samples studied using AFM is shown in Fig. 1. Ultrathin film of 20 nm thickness showed smooth surface with insignificant surface roughness. The root mean square (rms), calculated from AFM data, showed no clear dependence on the bilayers thickness up to 10 nm. A little decrease of the rms is observed when we reduce the bilayers thickness from 20 to 10 nm. After, the rms remains constant when decreasing the bilayers thickness from 10 to 1.2 nm. As reported elsewhere [10,11,13], amorphous Al_2O_3 blocks the ZnO crystal growth and forces the ZnO to renucleate on the Al_2O_3 surface. It should be noted that the surface roughness of nanolaminates was lower than that for 20 nm thick ZnO [10]. Transmittance spectra (Fig. 2) showed that all measured samples deposited on glass substrate were transparent in the range of 450–1100 nm. Nanolaminates with bilayer thickness of 1.2 nm and 2 nm did not show significant absorbance. Thus, it was difficult to distinguish ZnO absorbance from the substrate absorbance. The band gap value was calculated for samples with bilayer thickness of 20, 10 and 5.2 nm using the observed absorption edge.

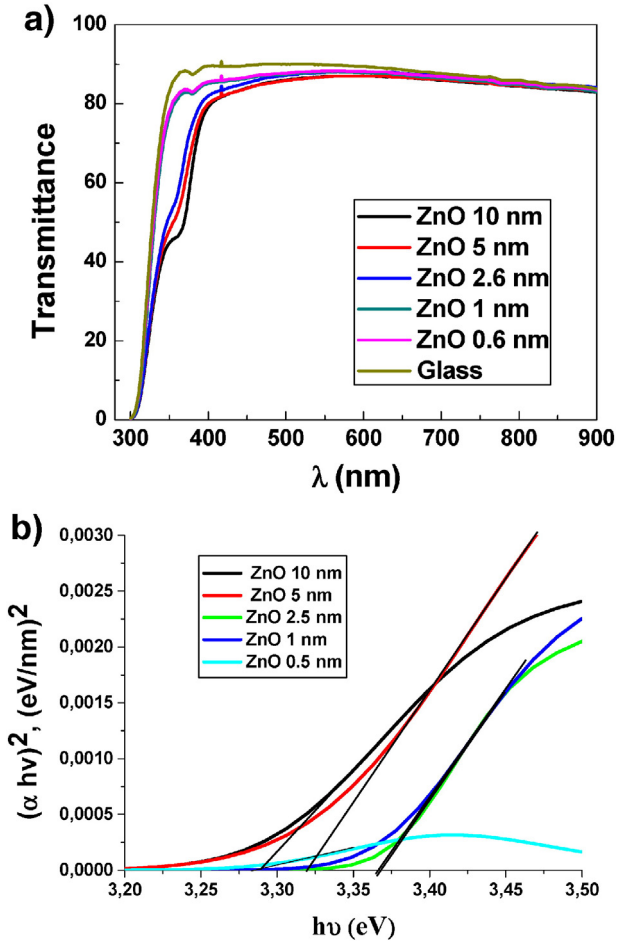

Fig. 2. a) Transmission spectra of Al_2O_3/ZnO nanolaminates with different bilayer thicknesses and (b) bandgap extraction from the plot of $(\alpha h\nu)^2$ as a function of photon energy ($h\nu$).

Absorption coefficient α is related to the transmittance of the sample T as [10,11]:

$$\alpha \cdot d = \ln\left(\frac{1}{T}\right) \quad (1)$$

where d is a thickness of the sample.

In order to simplify the calculation of the band gap values of the nanolaminates, an optical density OD ($OD = \alpha \times d$) was used [10,11].

The band gap value of the samples was calculated considering that Al_2O_3 is totally transparent and the observed absorption edge is related to ZnO layers. ZnO is known as a semiconductor with direct optical transitions. Therefore, the absorption coefficient α can be described by the following equation [10,11]:

$$\alpha = \frac{(h\nu - E_g)^{1/2}}{h\nu} \quad (2)$$

where $h\nu$ and E_g are a photon energy and a band gap values, respectively.

Considering Eqs. (1) and (2), from the plot $(OD \times h\nu)^2$ vs $h\nu$ band gap values E_g were graphically determined (Fig. 2b) in linear part of the absorption edge with respect to Eq. (2) and summarized in Table 2.

SE measurements were performed in order to determine optical dispersion of refractive index and extinction coefficient for Al_2O_3/ZnO nanolaminates. SE data for Al_2O_3/ZnO nanolaminates were analyzed by the multi-layer model [11]. In this study multi-layer model represented the structure of nanolaminates consisted from bilayers of Al_2O_3/ZnO. The Bruggeman effective media approximation was used to determine the fraction volume of Al_2O_3 and ZnO in the bilayers. The starting values of ZnO and Al_2O_3 optical dispersion was taken from "Complete Ease" software database. Single ZnO layer deposited on Si substrate with thickness of 250 nm was characterized by Critical Point Parabolic Band function [14]. This function is related to the electronic band-to-band transitions. Al_2O_3 optical constants in ultrathin nanolaminates were described using Cauchy dispersion function. The regression analysis was made by fixing the thickness of the stack layer of nanolaminate (20 nm) meanwhile coefficients in optical dispersion functions and volume fractions in bilayers were free fitting parameters. The mean square error (MSE) of nanolaminates modeling was from 7.3 to 23. The effective optical constants of nanolaminates differ depending on the bilayer thickness (Fig. 3). For comparison of refractive index values, the upper ZnO layers were taken. It can be seen, that the refractive index of ZnO decreases with the decrease of the single layer thickness in the range of 10 to 2.6 nm. The obtained results were compared with refractive index of 250 nm ZnO single layer, deposited on Si substrate. The decrease of ZnO refractive index, deposited on Al_2O_3 could be related to the change of the growth and the increase of the density of the deposited layers [11]. No constituent increase of refractive index was observed for nanolaminates with single ZnO layer thickness of 1 and 0.6 nm.

The extinction coefficients and band gap values have been used in order to analyze structural changes of nanolaminates depending on bilayers spacing obtained from SE and optical transmittance spectra.

Table 2
Band gap and Urbach energy of Al_2O_3/ZnO nanolaminates with different bilayer thicknesses.

Samples	E_g (eV) from transmittance	Eg (eV) from SE	Urbach energy (eV)
Al_2O_3/ZnO 20 (0.6/0.6 nm)	–	3.45	0.638623
Al_2O_3/ZnO 10 (1/1 nm)	–	3.42	0.473774
Al_2O_3/ZnO 4 (2.6/2.6 nm)	3.3	3.38	0.215752
Al_2O_3/ZnO 2 (5/5 nm)	3.25	3.39	0.062589
Al_2O_3/ZnO 1 (10/10 nm)	3.24	3.35	0.0826

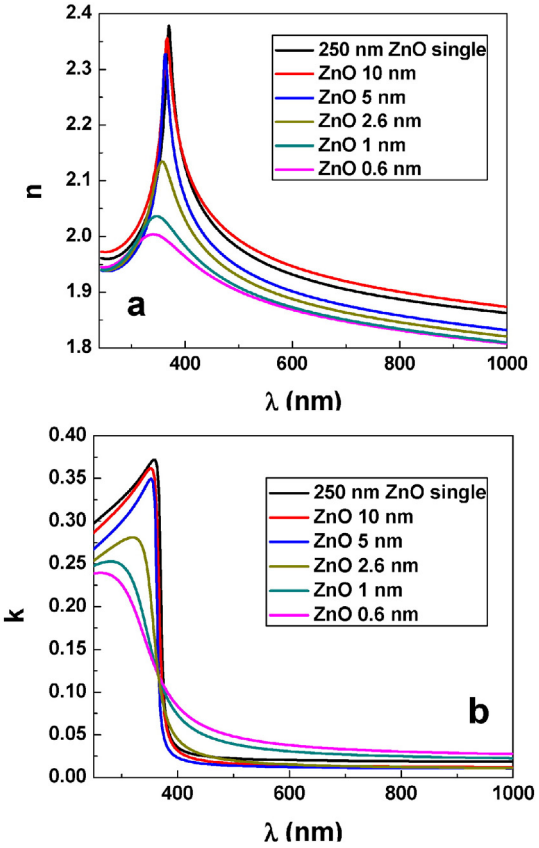

Fig. 3. Spectra of refractive index (a) and extinction coefficient (b) of ZnO single layers in Al_2O_3/ZnO nanolaminates with different bilayer thicknesses obtained by regression analysis of ellipsometric data.

To evaluate the band gap values, extinction coefficients of the top ZnO single layer were used. Extinction and absorption coefficients are related through following equation [11]:

$$\alpha = \frac{4 \cdot \pi \cdot k}{\lambda} \tag{3}$$

where α, k and λ are absorption, extinction coefficients and wavelength.

Extinction spectra of ZnO in Al_2O_3/ZnO nanolaminates, obtained from regression analysis of ellipsometric spectra are shown in Fig. 4. Blue shift of absorption edge and decreasing the extinction peaks were observed with the decrease of nanolaminate bilayer thickness (Fig. 3). The evaluated band gap values E_g were graphically calculated in linear part of the absorption edge, calculated according to Eq. (2), and summarized in Table 2.

In our previous work [11] we estimated average band gap value for nanolaminates with total thickness of 200 nm and single ZnO layer thickness of 10 nm and 2 nm. These values were 3.36 and 3.45, respectively, therefore the band gap values of ultrathin nanolaminates, grown at the beginning stage are lower than values for the samples with the total thickness 10 times higher.

The absorption edge of the samples lies in the range of 350–400 nm and was sharp for 20 and 10 nm bilayers thickness, meanwhile for 5.2, 2 and 1.2 nm bilayers thickness, the absorption edge was continuous, similar to high surface roughness or amorphous samples. [15]. In order to reveal the structural changes from point of degree of disorder with the decrease of bilayers thickness, the Urbach energy of ZnO was estimated [11]. Urbach tails in absorption peaks are observed when electron from state near the top of valence band is excited to a state near the bottom of conduction band. In the disordered (amorphous) system, electron energy states have different values of those for crystalline (regular) systems. The Urbach energy increases due to the change of the growth of ZnO over Al_2O_3 when the thickness of bilayer decreases from 20 to 1.2 nm. It demonstrates that the number of imperfections increases with the decrease of bilayer spacing and an amorphous structure was formed.

The Urbach tail has been graphically calculated from the linear part of $\ln(\alpha) \sim h\nu$ plot (Fig. 5). Absorption coefficient obtained from SE data (Fig. 4) have demonstrated that the Urbach tail values increase with the number of bilayers, pointing to the local states into the band gap and to the higher value of disorder [11]. The Urbach tail shows the concentration of local states close to conductance and valence bands.

Additionally, the PL of ultrathin nanolaminates was measured in the range of 365–800 nm and showed no emission for all set of samples. This result could have two possible explanations: (i) Samples are amorphous with not defined grain boundaries. In this case no exciton peaks are expected but defect level emission could be present and (ii) volume-to-surface aspect ratio of the samples is too low. In that case, the surface non radiative recombination is dominant.

Two theories were proposed to explain the results of ultrathin nanolaminates. The first initial idea was based on the growth mechanism proposed by Elam et al. [16] According to Elam et al., the substitution reaction of Zn with Al may happen:

$$Zn\text{–}OH^S + Al(C_2H_5)_3^g \rightarrow AlOH\text{–}C_2H_5^S + Zn(C_2H_5)_2^g\uparrow$$

where ZnO–OH and $Al(C_2H_5)_3$ are the substance on the surface and gas phase, correspondently. Due to this reason, the ratio of ZnO can be reduced and doping of ZnO may occur. The ZnO doping with Al was previously discussed by Moret et al. [17], Banerjee et al. [18] and Cheun

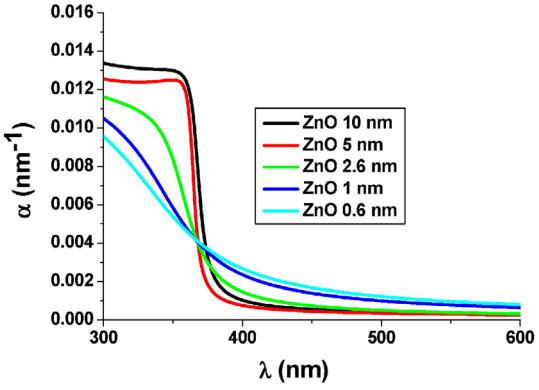

Fig. 4. Absorption spectra of ZnO single layers in Al_2O_3/ZnO nanolaminates with different bilayer thicknesses obtained by calculating from extinction spectra (Fig. 3b).

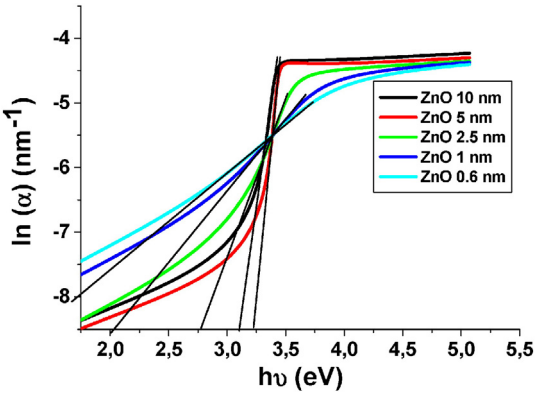

Fig. 5. Calculated Urbach tail from absorption coefficient for ZnO layers.

et al. [19]. The Al doping resulted in the increase of the bang gap value and the decrease of ZnO refractive index with the increase of Al doping ratio [20,21]. Comparing the band gap values and the refractive index, we can verify that the decrease of ZnO ratio can be observed only for 1 nm and 0.6 nm layers.

The second way to explain amorphous nature of ultrathin nanolaminates is the minimum thickness required to allow crystallization in a thin film. The proposed crystallization model for ultrathin layers and superlattices is taking into account the interface energies, the thickness of the layers, the melting point of the system, and the bulk amorphous crystallization temperature [22]. It was shown that exponential increase of the crystallization temperature leads to the decrease of the minimal thickness at which crystallization occurs. From XRD and previous HRTEM studies, [12] this bilayer thickness value was shown to be 2.5 nm for Al_2O_3/ZnO nanolaminates. So, we assume that this value is the point at which the crystallization process starts in Al_2O_3/ZnO nanolaminates.

4. Conclusion

In summary, optical and structural properties of ultrathin Al_2O_3/ZnO nanolaminates, deposited on Si and glass substrates have been studied. Regression analysis of ellipsometric spectra have shown that absorption peak decrease and blue shifted with the decrease of bilayers thickness in the stack. Such behavior reveals the formation of disordered structures with decreasing the thickness of bilayers. The degree of disordering has been analyzed by calculating the Urbach tail at the band edge of the absorption spectra of Al_2O_3/ZnO nanolaminates. Analysis of Urbach energy have shown that structures with bilayer spacing of 2 nm and 1.2 nm have noticeably higher Urbach energy values that structures with thicker bilayers thicknesses. The evaluated Urbach energy value of about 0.5 eV and higher for ZnO layer was the indication of the amorphous structure formation. These results were supported by XRD data, no peaks pointing to crystalline structure have been found, as well as the absence of PL exitonic peaks, which was detected in thicker samples [10,11]. Finally, we conclude that on the basis of the analysis of optical methods such as transmission, spectroscopic ellipsometry and photoluminescence of ultrathin nanolaminates, the amorphous nature of them has been proven. These results allowing not only to determine optical properties of Al_2O_3/ZnO nanolaminates but also to get some inside on the formation processes of ultrathin films of Al_2O_3/ZnO.

Acknowledgments

The research was supported by Fotonika-LV (FP7-Reg Pot-2011-1, contract nr. 285912), BIOSENSORS-AGRICULT (FP7-PEOPLE-2012-IRSES, contract nr. 318520) and by a grant (No. TAP LZ-3/2015) from the Research Council of Lithuania.

References

[1] A. Paracchino, V. Laporte, K. Sivula, M. Grätzel, E. Thimsen, Highly active oxide photocathode for photoelectrochemical water reduction, Nat. Mater. 10 (2011) 456–461.
[2] J. Elias, M. Bechelany, I. Utke, R. Erni, D. Hosseini, J. Michler, L. Philippe, Urchin-inspired zinc oxide as building blocks for nanostructured solar cells, Nano Energy 1 (2012) 696–705.
[3] M. Jędrzejewska-Szczerska, P. Wierzba, A.A. Chaaya, M. Bechelany, P. Miele, R. Viter, A. Mazikowski, K. Karpienko, M. Wróbel, ALD thin ZnO layer as an active medium in a fiber-optic Fabry–Perot interferometer, Sensors Actuators A Phys. 221 (2015) 88–94.
[4] R. Viter, V. Khranovskyy, N. Starodub, Y. Ogorodniichuk, S. Gevelyuk, Z. Gertnere, N. Poletaev, R. Yakimova, D. Erts, V. Smyntyna, A. Ubelis, Application of room temperature photoluminescence from ZnO nanorods for *Salmonella* detection, IEEE Sensors J. 14 (2014) 2028–2034.
[5] A.A. Chaaya, M. Bechelany, S. Balme, P. Miele, ZnO 1D nanostructures designed by combining atomic layer deposition and electrospinning for UV sensor applications, J. Mater. Chem. A 2 (2014) 20650–20658.
[6] S. Cabello-Aguilar, S. Balme, A.A. Chaaya, M. Bechelany, E. Balanzat, J.-M. Janot, C. Pochat-Bohatier, P. Miele, P. Dejardin, Slow translocation of polynucleotides and their discrimination by [small alpha]-hemolysin inside a single track-etched nanopore designed by atomic layer deposition, Nanoscale 5 (2013) 9582–9586.
[7] T.W. Barbee Jr., Nano-laminates: a new class of materials for aerospace applications, Aerospace Conference, 2003, Proceedings. 2003 IEEE 2003, pp. 4_1745–1744_1754.
[8] K. Ellmer, A. Klein, B. Rech (Eds.), Transparent Conductive Zinc Oxide: Basics and Applications in Thin Film Solar Cells, Springer Ser. Mater. Sci., 2008, 104, Springer, 2008.
[9] H. Fujiwara, Principles of Spectroscopic Ellipsometry, Spectroscopic Ellipsometry, John Wiley & Sons, Ltd., 2007 81–146.
[10] A. Abou Chaaya, R. Viter, M. Bechelany, Z. Alute, D. Erts, A. Zalesskaya, K. Kovalevskis, V. Rouessac, V. Smyntyna, P. Miele, Evolution of microstructure and related optical properties of ZnO grown by atomic layer deposition, Beilstein J. Nanotechnol. 4 (2013) 690–698.
[11] A.A. Chaaya, R. Viter, I. Baleviciute, M. Bechelany, A. Ramanavicius, Z. Gertnere, D. Erts, V. Smyntyna, P. Miele, Tuning optical properties of Al_2O_3/ZnO nanolaminates synthesized by atomic layer deposition, J. Phys. Chem. C 118 (2014) 3811–3819.
[12] R. Raghavan, M. Bechelany, M. Parlinska, D. Frey, W.M. Mook, A. Beyer, J. Michler, I. Utke, Nanocrystalline-to-amorphous transition in nanolaminates grown by low temperature atomic layer deposition and related mechanical properties, Appl. Phys. Lett. 100 (2012).
[13] J.W. Elam, S.M. George, Growth of ZnO/Al_2O_3 alloy films using atomic layer deposition techniques, Chem. Mater. 15 (2003) 1020–1028.
[14] D.E. Aspnes, Modulation Spectroscopy/Electric Field Effects on the Dielectric Function of Semiconductors, North-Holland, 1980 109–154.
[15] Y.-y. Liu, S.-y. Yang, G.-x. Wei, H.-s. Song, C.-f. Cheng, C.-s. Xue, Y.-z. Yuan, Electrical and optical properties dependence on evolution of roughness and thickness of Ga: ZnO films on rough quartz substrates, Surf. Coat. Technol. 205 (2011) 3530–3534.
[16] J.W. Elam, Z.A. Sechrist, S.M. George, ZnO/Al_2O_3 nanolaminates fabricated by atomic layer deposition: growth and surface roughness measurements, Thin Solid Films 414 (2002) 43–55.
[17] M. Moret, A. Abou Chaaya, M. Bechelany, P. Miele, Y. Robin, O. Briot, Atomic layer deposition of zinc oxide for solar cell applications, Superlattice. Microst. 75 (2014) 477–484.
[18] P. Banerjee, W.-J. Lee, K.-R. Bae, S.B. Lee, G.W. Rubloff, Structural, electrical, and optical properties of atomic layer deposition Al-doped ZnO films, J. Appl. Phys. 108 (2010).
[19] H. Cheun, C. Fuentes-Hernandez, J. Shim, Y. Fang, Y. Cai, H. Li, A.K. Sigdel, J. Meyer, J. Maibach, A. Dindar, Y. Zhou, J.J. Berry, J.-L. Bredas, A. Kahn, K.H. Sandhage, B. Kippelen, Oriented growth of Al_2O_3:ZnO nanolaminates for use as electron-selective electrodes in inverted polymer solar cells, Adv. Funct. Mater. 22 (2012) 1531–1538.
[20] H. Benzarouk, A. Drici, M. Mekhnache, A. Amara, M. Guerioune, J.C. Bernède, H. Bendjffal, Effect of different dopant elements (Al, Mg and Ni) on microstructural, optical and electrochemical properties of ZnO thin films deposited by spray pyrolysis (SP), Superlattice. Microst. 52 (2012) 594–604.
[21] S.W. Xue, X.T. Zu, W.G. Zheng, H.X. Deng, X. Xiang, Effects of Al doping concentration on optical parameters of ZnO:Al thin films by sol–gel technique, Phys. B Condens. Matter 381 (2006) 209–213.
[22] M. Zacharias, P. Streitenberger, Crystallization in the limit of ultra thin layers — a new crystallization model, Mater. Res. Symp. Proc. 638 (2001) F6.2.1–F6.2.6.